

Tuning the response of long-period fiber gratings for chemical sensing applications

Hannes Hochreiner^a, Michael Cada^b, Peter D. Wentzell^a

^aTrace Analysis Research Centre, Dept. of Chemistry, Dalhousie University, Halifax, NS, Canada B3H 4J3;

^bDept. of Electrical and Computer Engineering, Dalhousie University, Halifax, NS, Canada, B3J 1Z1;

ABSTRACT

In recent years, the use of long-period gratings (LPGs) as fiber optic chemical sensors has been proposed by several authors. Such implementations take advantage of the changes in the LPG transmittance characteristics with ambient refractive index and may make use of a polymer coating to enhance chemical selectivity and sensitivity. While technically feasible, these designs are subject to fairly rigid constraints related to the optical characteristics of the fiber and grating, as well as the thickness and refractive index of the chemically selective polymer. Compromises in design may lead to sub-optimal sensor performance in terms dynamic range, sensitivity, linearity, stability and response time. In this work, LPG sensor designs based on one-, two- and three-layer geometries are explored, where the outer layer is the chemically selective polymer and the properties of the other layers (thickness, refractive index) can be adjusted. It is demonstrated through calculations based on a hybrid mode model that the use of more than one layer greatly enhances the flexibility of sensor design and allows the response characteristics to be tuned for optimal performance. A case study is used to illustrate how the same sensor can be optimized for several factors, including linearity, range, sensitivity, and stability.

Keywords: long-period grating, fiber optic sensor, chemical sensor, refractive index, hybrid mode model

1. INTRODUCTION

Fiber optic chemical sensors offer many advantages over other modes of sensing for monitoring chemical environments and have been the subject of research and development for several decades. Most of these optical sensing applications rely on the measurement of absorption or luminescence as the mode of transduction. While these will no doubt continue to be the primary modes of measurement, they suffer from a number of disadvantages, including the need for native absorption or fluorescence (or appropriate modification of the analyte with a chromophore or fluorophore) and often poor selectivity and limited multianalyte capabilities. The ideal sensor would be universally responsive and yet still exhibit the potential for selective detection of analytes. One possible alternative to the use of traditional modes of fiber optic sensing in chemistry is the use of optical fiber long-period grating (LPG) sensors.

LPGs are optical fibers in which a short length (typically a few centimeters) of the core is subjected to a periodic modulation (with a fixed or changing period) of the refractive index, typically with a period of a few hundred microns. This leads to a coupling between the core mode and co-propagating cladding modes and results in the attenuation of certain wavelength regions (bands) in the transmission spectrum of the fiber. LPGs are related to fiber Bragg gratings (FBGs), which have shorter periods and lead to coupling between the core mode and counter-propagating modes. A particular feature of LPGs that makes them useful as sensors is the sensitivity of the transmission spectrum to changes in certain environmental factors such as strain, bending, temperature and ambient refractive index.¹ The sensitivity to refractive index (RI) is of particular interest from a chemical sensing perspective, since RI is a universal property that can be monitored for all chemical environments and

Further author information:

H.H.: E-mail: hannes@hochreiner.net

M.C.: E-mail: michael.cada@dal.ca

P.D.W.: E-mail: peter.wentzell@dal.ca, Telephone: +1 (902) 494 3708

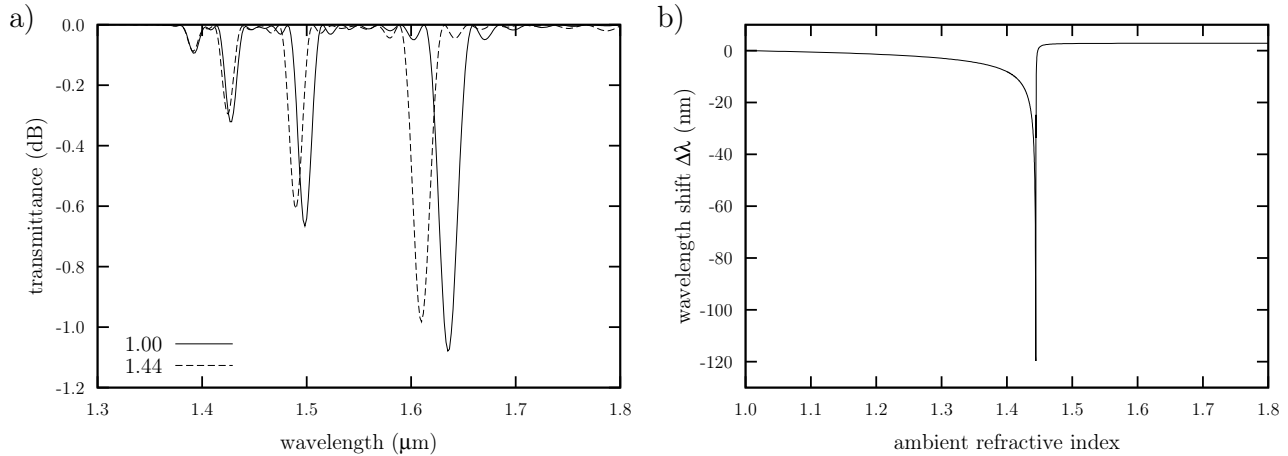


Figure 1. a) Spectra of a bare LPG sensor element. The numbers in the legend refer to the ambient RI. b) Theoretically expected shift of the peak around 1630 nm calculated using the Bragg condition.

depends on chemical composition. Although this opens the door for chemical sensing applications of LPGs, a number of challenges related to the sensitivity, selectivity and response characteristics of these devices remain to be met. The purpose of this work is to demonstrate, through the use of theoretical models, how sensor design elements can be modified to tune the response of these devices to optimize their analytical performance.

1.1 Long-period gratings as chemical sensors

Figure 1 a) shows the calculated transmission spectra for a typical LPG under two different conditions of ambient RI. An important limitation of these kinds of measurements is that the ambient RI must be smaller than the RI of the cladding (*i.e.* $n_{ambi} < n_{clad}$) in order for such changes to be observed. Figure 1 b) shows a plot of the wavelength shift of the large attenuation band at about 1630 nm as a function of the ambient RI. Note that the LPG is very sensitive to RI changes, but only over a small region near the RI of the cladding.

Before the LPG can be used as a chemical sensor, a number of issues need to be addressed, most notably those related to sensitivity and selectivity. Although LPGs are quite sensitive to small changes in ambient RI at values close to n_{clad} , the RI of the chemical environment is a bulk property and significant changes require relatively large changes in the chemical composition, making the direct monitoring of RI unsuitable for detecting low concentrations of analytes. Moreover, since the RI of the chemical environment can be altered by the addition of any chemical species, there is no specificity for the analyte. Another problem is that the most common ambient environments, water and air, will have RI values much lower than that of the cladding, meaning that RI changes will not be detected in the transmission spectrum.

To overcome these problems, one solution that has been proposed and implemented is to coat the LPG fiber with a thin layer of polymer.² This serves several purposes. First, the RI of the polymer can (in principle) be “tuned” to a value smaller than but close to that of the cladding for maximum sensitivity. Second, the polymer can serve to partition analytes in the surrounding medium into a smaller volume through solid phase microextraction (SPME), allowing a greater sensitivity to be achieved through the higher concentration in the polymer layer. Finally, the nature of the polymer can be chosen to permit differential extraction analytes based on their properties, thus allowing some level of selectivity to be achieved.

This type of sensor design, which will be referred to as the one-layer sensor because it employs a single polymer layer between the cladding and the ambient environment, greatly expands the sensing capabilities over those of the bare fiber. Such sensors have been demonstrated to respond in both liquid and gas phase environments,^{3,4} although the latter is more amenable to practical sensing applications because there are fewer problems with polymer swelling, response time, reversibility, leaching of polymer materials and other such phenomena. This approach shows promise, but there are still a number of design challenges to be met, as discussed in the next section.

1.2 Design challenges for one-layer sensors

Although the basic principles of the one-layer LPG chemical sensor have been demonstrated, there remain significant hurdles to be overcome. One of these concerns the nature of the response itself. There are two obvious modes of operation of such sensors that differ in the parameter that is measured. One method of transduction would be to measure the wavelength shift of one (or more) of the attenuation bands in the transmission spectrum. Although this is intuitively appealing and should result in a largely monotonic response, it is not very practical, since it requires a tunable laser source, delays for scanning, and peak identification capability. A technically simpler alternative is to use a source with a wavelength fixed near one of the attenuation bands and record the attenuation as the band shifts position. In either case, the response is expected to be nonlinear with concentration and appropriate calibration methods will be needed to deal with this.

A second issue is that of selectivity. Although polymer coatings can be developed with different partition coefficients for different chemical species, complete specificity for one analyte is not easily achieved. For this reason, it is likely that such sensors would have to be implemented as sensor arrays, using the complementary selectivities of multiple sensors, each with a different polymer coating, to enhance specificity for a single analyte or class of analytes through chemometric calibration methods. Such arrays would also be useful in handling the nonlinear response characteristics described in the preceding paragraph. It should also be kept in mind that the design of polymer coatings for one-layer sensors is also subject to constraints on the RI ($n_{clad} \cong n_{poly}$), which is an additional design restriction. Also, practical or mass transport considerations may place boundaries on the thickness of the polymer coating, adding additional constraints. It is desirable, if possible, to remove some of these constraints to simplify the design of the chemically selective polymers as much as possible.

A third important issue, and the principal focus of this work, is the concentration sensitivity of the LPG sensor. Although the response of the LPG to changes in the polymer RI can be predicted, the response to changes in the analyte concentration in the ambient environment (*i.e.* the chemical sensitivity) depends on a number of factors that include: (1) the partition coefficient of the analyte between the polymer and the surrounding environment, (2) the effect of analyte concentration on polymer RI (*i.e.* dn_{poly}/dC), and (3) the thickness of the polymer. Because of the nature of one-layer LPG sensors, the useful response is confined to fixed refractive index intervals and this could potentially limit the utility of the sensor. If the analyte concentration range corresponds to a RI window that is outside the response range of the sensor, no appreciable signal will be observed. If the analyte RI window contains the response range, but is wider than this range, the dynamic range of the sensor will be limited and a signal will not be observed over the full range of concentrations. On the other hand, if the analyte RI window is narrower than the response range, sensitivity is sub-optimal and the limit of detection (LOD) may be too high. Ideally, one would like to be able to match the RI changes occurring in the polymer to the response window of the LPG. Since it is quite difficult to change the properties of the polymer, which is already subject to a number of constraints (nominal RI, selectivity, thickness), in a desired way, the alternative is to tune the response of the LPG sensor. In the context of a one-layer sensor, this is difficult to do since the existing constraints in the design do not favor incorporating great flexibility in the sensor response.

An alternative to the one-layer sensor, which allows greater design flexibility and permits effective matching of sensor response window to the expected RI changes in the polymer, is the multilayer sensor. In these designs, one or more additional layers is interposed between the cladding and the polymer layer. Although this incorporates an additional level of complexity in the construction of the sensor, it also greatly enhances the flexibility of the sensor by adding new design variables (*i.e.* the RI and thickness of the interposing layers). This allows the response characteristics to be more easily controlled and relaxes some of the constraints on the chemically sensitive polymer layer. In this work, the design and response characteristics of two- and three-layer sensors are considered in the context of chemical sensing applications.

1.3 LPG models

The study of polymer coated LPGs and their use as sensors is a relatively new field. Therefore, it comes as no surprise that the vast majority of studies are limited to simplest case, *i.e.* a one-layer sensor. James *et al.*⁵ recently carried out a review of fiber optic sensors with thin coatings that includes a section on LPG sensors. A more detailed discussion of the relevant literature is provided here to put this work into an appropriate context.

In 2002, Rees *et al.*² first investigated the behavior of LPGs with thin film overlays in an experiment where a Langmuir-Blodgett technique was used to deposit tricosenoic acid. The film thickness was determined as the product of the number of deposition passes and the thickness of one layer, which was given as 2.6 nm. The refractive index of the overlay material was reported to be 1.57. The shift of the peaks in the LPG spectrum was qualitatively discussed in terms of the average refractive index of the medium surrounding the fiber. It was pointed out that the overlays enabled new modes of operation of LPG elements as it could be shown that the peak position was now also sensitive to refractive indices higher than that of the cladding. Similar experiments and conclusions were presented by Ishaq *et al.*⁶ in 2005.

In the same year, del Villar *et al.*⁷ presented a theoretical explanation of the sensitivity enhancement effect based on the transition of cladding modes from being guided in the cladding to being guided in the overlay. The linearly polarized (LP) mode structures of the geometries of interest were obtained using a transfer matrix approach in the radial direction. The theoretical results were supported by experiments using electrostatic self-assembly to produce 0.5 nm thick layers of [PDDA⁺/PolyR-47⁻]. The refractive index of the overlay material was estimated to be 1.62. A more detailed paper by the same researchers⁸ was published shortly afterwards. The mode structures were shown over a larger effective refractive index interval in order to demonstrate the transition of several cladding modes from the cladding to the overlay and the reorganization of the remaining cladding modes to reconstruct the mode structure present before the transition. Furthermore, it was demonstrated how the mode fields of the cladding modes change as their effective refractive index changes from the initial value to a value similar to the original value of the next lower cladding mode. It was also shown how the cladding mode shift occurs for thinner overlays as the refractive index of the overlay is increased. Extending their analysis to coatings with absorbing layers (complex refractive index), del Villar *et al.*⁹ showed — experimentally and theoretically — that additional phenomena are seen in this case. As the modes transition into the overlay, the complex part of their propagation constants increases, which leads to a vanishing of the corresponding resonance peak in the spectrum. It was also found that the peaks no longer transition in order (i.e. it is not always the lowest order peak that becomes guided by the overlay).

Using LPGs with thin overlays, Wang *et al.*¹⁰⁻¹² investigated the dependence of the peak shift of the cladding mode resonances on the mode order, the ambient refractive index and the overlay thickness. For the theoretical analysis, an LP model was used, while the experiments were carried out using ionic self-assembled multi-layers of refractive indices ranging from 1.67 - 1.72. The refractive index of the overlays was controlled by varying their composition and pH. The investigated overlay thickness was between zero and 60 nm.

In 2006, del Villar *et al.*¹³ extended their previous analysis using a hybrid mode model. It was shown that the transition of the odd and even hybrid modes occur at slightly different overlay thickness. Comparing the LP model with the hybrid mode model for the case of thin overlays, it was concluded that the largest error is to be expected when the effective refractive index of the cladding modes is close to the effective refractive index of the core mode. It was pointed out that if the weak guidance condition is not fulfilled, low order modes should show a two-step transition rather than the one step transition predicted by the LP model. For the case of overlay materials having a complex refractive index, a vanishing of the modes during the transition was predicted as the imaginary part of the propagation constant of the mode would increase.

Two-layer sensors have so far attracted much less attention. In a paper by del Villar *et al.*,¹⁴ it was pointed out that a high refractive index overlay can be sandwiched between the cladding and a low refractive index overlay to enhance the sensitivity of the LPG to changes in the low refractive index overlay. The resulting five layer geometry (core, cladding, first and second overlay, ambient environment) was theoretically analyzed using a hybrid mode model. It was noted that on increasing the thickness of the low refractive index overlay, the response will become increasingly similar to the case of an LPG with an infinitely extended low refractive index overlay.

Another paper by del Villar *et al.*¹⁵ examined the sensitivity change of an LPG when varying the refractive index of a high refractive index overlay using a hybrid mode model. The analysis was similar to the one undertaken in this work. However, while in the article the authors limited their investigation to one high refractive index overlay, this report will extend the analysis to include also low refractive index overlays and multi-overlay geometries.

Significant contributions to this field were also made by Cusano *et al.* by publishing a theoretical analysis based on an LP mode model supported by experimental data.¹⁶ A study of the dependence of the sensitivity on the overlay thickness was presented. It was mentioned that high refractive overlays offer the opportunity to adjust the refractive index interval of highest sensitivity of the LPG sensor element. An implementation of these principles were presented shortly afterwards in the form of an LPG coated with syndiotactic polystyrene, which was used as a sensor for chloroform in water.³ After the introduction of this sensor, another article¹⁷ included a more detailed characterization and extensive theoretical work. In a subsequent paper,¹⁸ more details on the mode fields were presented. It was shown that on transition, the higher order modes assume a mode field similar to that of the next lower mode and the mode field of the transitioning mode shifts into the overlay. In a very recent article,¹⁹ the authors present an analysis of the sensitivity of LPG coated with high refractive index polymers. In this work, special attention was paid to the dependence of sensitivity on the overlay thickness and the mode order.

2. METHODS

2.1 Theoretical model

Modal models based on linearly polarized (LP) modes (*i.e.* employing the weak guidance approximation) have been shown to yield good results for simulating LPGs in fibers surrounded by an infinite medium.²⁰ However, as mentioned in the last section, considerable differences from the more accurate hybrid mode model can be found with some overlay structures.²¹ Therefore, the computationally more involved hybrid mode model was used in this study.

The field components of the hybrid modes in a homogeneous medium can be described in cylindrical coordinates as^{21,22}

$$E_z = [AC_\nu(\gamma r) + BD_\nu(\gamma r)] \cos(\nu\Phi + \phi), \quad (1)$$

$$H_z = [CC_\nu(\gamma r) + DD_\nu(\gamma r)] \cos(\nu\Phi + \psi), \quad (2)$$

$$E_r = \frac{i\beta_{\nu j}}{s\gamma^2} \left(\frac{\partial}{\partial r} E_z + \frac{k_0 Z_0 u^2}{\beta_{\nu j}} \frac{\partial}{r \partial \Phi} H_z \right), \quad (3)$$

$$E_\Phi = \frac{i\beta_{\nu j}}{s\gamma^2} \left(\frac{\partial}{r \partial \Phi} E_z - \frac{k_0 Z_0 u^2}{\beta_{\nu j}} \frac{\partial}{\partial r} H_z \right), \quad (4)$$

$$H_r = \frac{i\beta_{\nu j}}{s\gamma^2} \left(\frac{\partial}{\partial r} H_z - \frac{k_0 e^2}{Z_0 \beta_{\nu j}} \frac{\partial}{r \partial \Phi} E_z \right), \quad (5)$$

$$H_\Phi = \frac{i\beta_{\nu j}}{s\gamma^2} \left(\frac{\partial}{r \partial \Phi} H_z + \frac{k_0 e^2}{Z_0 \beta_{\nu j}} \frac{\partial}{\partial r} E_z \right), \quad (6)$$

with

$$\begin{aligned} C_\nu = J_\nu, D_\nu = Y_\nu, \gamma = \sqrt{k_0^2 n^2 - \beta_{\nu j}^2}, s = 1 \quad \text{when } \beta_{\nu j} < k_0 n, \\ C_\nu = I_\nu, D_\nu = K_\nu, \gamma = \sqrt{\beta_{\nu j}^2 - k_0^2 n^2}, s = -1 \quad \text{when } \beta_{\nu j} > k_0 n, \end{aligned} \quad (7)$$

where $e = \sqrt{\epsilon/\epsilon_0}$ and $u = \sqrt{\mu/\mu_0}$ and ϵ and μ are the permittivity and the permeability, while the zero subscripts indicate the respective quantity in free space. The variable k_0 is the free space wave vector defined as $2\pi/\lambda$, where λ is the free space wavelength, $\beta_{\nu j}$ is the propagation constant of the mode of order ν , and n is the refractive index of the medium. A , B , C and D are the field expansion coefficients of the mode in the medium; Z_0 is the impedance of free space. J_ν , Y_ν and I_ν , K_ν are the Bessel function of the first and second kind of order ν and their respective modified versions.

To derive the characteristic equation, it is convenient to choose four of the above six field components and write them in matrix form

$$\begin{pmatrix} E_z \\ H_\Phi \\ H_z \\ E_\Phi \end{pmatrix} = \begin{pmatrix} C_\nu & D_\nu & 0 & 0 \\ \frac{ik_0 e^2}{Z_0 s \gamma} C'_\nu & \frac{ik_0 e^2}{Z_0 s \gamma} D'_\nu & -\frac{\nu \beta}{s \gamma^2 r} C_\nu & -\frac{\nu \beta}{s \gamma^2 r} D_\nu \\ 0 & 0 & C_\nu & D_\nu \\ -\frac{\nu \beta}{s \gamma^2 r} C_\nu & -\frac{\nu \beta}{s \gamma^2 r} D_\nu & -\frac{ik_0 Z_0 u^2}{s \gamma} C'_\nu & -\frac{ik_0 Z_0 u^2}{s \gamma} D'_\nu \end{pmatrix} \begin{pmatrix} A \\ B \\ C \\ D \end{pmatrix} = T \begin{pmatrix} A \\ B \\ C \\ D \end{pmatrix}. \quad (8)$$

Imposing continuity of the fields at the interface between two layers as the boundary condition, the field expansion coefficients of two adjacent layers can be related by a transfer matrix in the radial direction:

$$T_n \begin{pmatrix} A_n \\ B_n \\ C_n \\ D_n \end{pmatrix} = T_{n+1} \begin{pmatrix} A_{n+1} \\ B_{n+1} \\ C_{n+1} \\ D_{n+1} \end{pmatrix} \quad (9)$$

By substitution, a structure with an arbitrary number of layers can be built up. In the final expression, the field expansion coefficients of the first layer will be related to the coefficients in the last layer.

$$\begin{pmatrix} A_0 \\ B_0 \\ C_0 \\ D_0 \end{pmatrix} = T_0^{-1} T_1 T_1^{-1} T_2 \dots T_{N-1}^{-1} T_N \begin{pmatrix} A_N \\ B_N \\ C_N \\ D_N \end{pmatrix} = M \begin{pmatrix} A_N \\ B_N \\ C_N \\ D_N \end{pmatrix} \quad (10)$$

Demanding that the fields be finite ($B_0 = 0$, $D_0 = 0$, $A_N = 0$, $C_N = 0$), the characteristic equation for the structure is obtained

$$0 = M(2, 2)M(4, 4) - M(2, 4)M(4, 2). \quad (11)$$

Subsequently, the field expansion coefficients for each layer can be calculated and the fields can be normalized to carry the same power (P_0)²³

$$P_0 = 1/2 \operatorname{Re} \int_0^{2\pi} d\phi \int_0^\infty r dr (E_r H_\phi^* - H_r^* E_\phi). \quad (12)$$

Coupled mode theory (CMT) was used to approximate the effect of the grating. The index variation of the grating (Δn) was modeled as the product of three functions²⁰

$$\Delta n(r, \phi, z) = \sigma_a(z) S(z) P(r, \phi). \quad (13)$$

Here σ_a is an apodisation function, which in the case of this study was set to 1. S refers to a longitudinal periodic function that consists of a constant (s_0) and a variable (s_1) part

$$S(z) = s_0 + s_1 \cos\left(\frac{2\pi}{\Lambda} z\right). \quad (14)$$

In this equation Λ is the period of the grating. P represents the maximum induced index change of the grating.

The complete CMT formulations includes longitudinal and transversal coupling. However, since the longitudinal field components are orders of magnitude smaller than the transversal components, only the transversal coupling coefficient will be considered in the following calculations. Furthermore, the back-propagating modes can be neglected, as the large period of the grating will not allow significant coupling of the core mode with these modes. The CMT equations therefore simplify to²³

$$\frac{dA_\mu}{dz} = i \sum_\nu A_\nu(z) K_{\nu\mu}^t(z) \exp(i(\beta_\nu - \beta_\mu)z), \quad (15)$$

where

$$K_{\nu\mu}^t = \frac{\omega}{4P_0} \int_0^{2\pi} d\phi \int_0^\infty r dr \Delta\epsilon(r, z) \mathbf{E}_\nu^t(r, \phi) \mathbf{E}_\mu^{t*}(r, \phi). \quad (16)$$

For simplicity, it was assumed that there is no azimuthal variation. The azimuthal integral in Equation (16) can therefore be expressed as²³

$$\int_0^{2\pi} d\phi \exp(i(\nu - \mu)\phi) = 2\pi \delta_{\nu\mu}, \quad (17)$$

where $\delta_{\nu\mu}$ is the Kronecker delta function, which is 1 for $\nu = \mu$ and zero otherwise. It is easily seen from Equation (17) that only interactions between the core mode and cladding modes of the same order as the core mode ($\nu = 1$) have to be considered. The permittivity variation ($\Delta\epsilon$) can be expressed in terms of the refractive index variation using the approximate equation

$$\Delta\epsilon(r, \phi, z) \simeq 2\epsilon_0 n_0(r) \Delta n(r, \phi, z) \quad (18)$$

where n_0 is the original refractive index of the layer.²⁰ Substituting Equation (13) and (18) into Equation (16) the coupling coefficient can be expressed as

$$K_{\nu\mu} = \sigma(z) \left[s_0 + s_1 \cos\left(\frac{2\pi}{\Lambda} z\right) \right] \zeta_{\nu\mu},$$

$$\zeta_{\nu\mu} = \frac{\omega\epsilon_0}{2P_0} \int_0^{2\pi} d\phi \int_0^\infty r dr n_0(r, z) P(r, \phi) \mathbf{E}_\nu^t(r, \phi) \mathbf{E}_\mu^{t*}(r, \phi). \quad (19)$$

The ordinary differential equation (ODE) system implicitly defined in Equation (15) can then be written out in an efficient way by neglecting very small terms²¹

$$\begin{pmatrix} \frac{d}{dz} A_{11} \\ \frac{d}{dz} A_{12} \\ \vdots \\ \frac{d}{dz} A_{1N} \end{pmatrix} = \begin{pmatrix} Q_{11} & V_{12,11} & \cdots & V_{1N,11} \\ V_{11,21} & Q_{12} & \cdots & V_{1N,12} \\ \vdots & \vdots & \ddots & \vdots \\ V_{11,1N} & V_{12,1N} & \cdots & Q_{1N} \end{pmatrix} \begin{pmatrix} A_{11} \\ A_{12} \\ \vdots \\ A_{1N} \end{pmatrix},$$

$$Q_{1j} = -i\sigma(z) s_0 \zeta_{1j,1j},$$

$$V_{1j,1k} = -i\sigma(z) \frac{s_1}{2} \zeta_{1j,1k} \exp\left[-iz\left(\beta_{1j} - \beta_{1k} \pm \frac{2\pi}{\Lambda}\right)\right]. \quad (20)$$

The plus/minus in the exponent is selected to give the smaller number in the exponent and thereby the stronger coupling. The factor yielded with the other sign is neglected. Assuming that the grating is located far from the light source, the initial amplitudes can be set to $A_{11}(0) = 1$, $A_{12\dots 1N}(0) = 0$. After solving the ODE system, the transmittance (T_{LPG}) can be obtained as

$$T_{LPG} = \frac{A_{11}(L)^2}{A_{11}(0)^2}. \quad (21)$$

2.2 Simulation studies

For the simulation studies, fiber parameters representative of commercially available fibers were used. The core was assumed to have a radius $4.1 \mu\text{m}$ and a refractive index of 1.45. For the cladding, a radius of $62.5 \mu\text{m}$ and a refractive index of 1.4447 was used. For simplicity, the wavelength dependence of the fiber materials and the coating polymers was neglected. The grating period is $500 \mu\text{m}$ and its length 25 mm. The maximum induced refractive index change (P) was set to 1×10^{-4} . The grating was assumed to be sinusoidal ($s_0 = s_1 = 1$) and confined to the core.

3. RESULTS & DISCUSSION

To study the response of LPG sensor elements, one- to three-layer sensors were simulated. The sensors were assumed to operate in air, *i.e.* the refractive index of the surrounding medium was set to 1.0. It was found to be helpful to prepare plots of the effective refractive index of different cladding modes versus either wavelength or the refractive index change of the outermost layer at fixed wavelength. These plots will be referred to in this work as a mode structure plot. An example can be seen in Figure 2 a). Each curve represents a different mode (lower order modes higher in the graph) and can be thought of as being associated with an attenuation band in the transmission spectrum. Whether a mode gives actually rise to a peak in the spectrum depends on the magnitude of the different field components in the center of the fiber. The sigmoidal transitions in the effective refractive index indicate the regions of refractive index of the outermost layer over which the changes in the

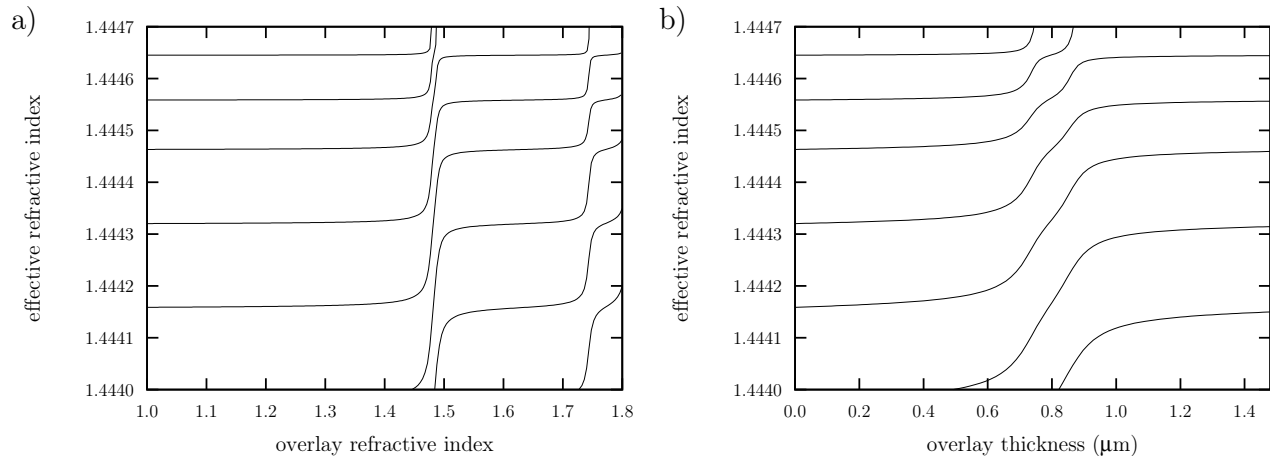


Figure 2. a) Mode structure plot of a one-layer sensor. The layer thickness is $1 \mu\text{m}$. The values of the abscissa refer to the refractive index of the overlay. b) Mode structure plot of a one-layer sensor. The refractive index of the overlay is 1.5. The values of the abscissa refer to the overlay thickness.

transmission spectrum will take place. These changes will normally involve shifts in wavelength minima as well as decreases or increases in the magnitude of the attenuation. Although the exact nature of the spectral changes depend on a number of system parameters, the mode structure plots are very useful from a design perspective because they help to identify the responsive regions of the LPG. Mode structure plots were prepared where the refractive index of the outermost coating was varied from 1.0-1.8. This interval was believed to cover all cases relevant in the context of this project. Since there is a multitude of cladding modes supported by all the investigated structures, only a few of the lowest order modes are shown. The other parameters (*i.e.* the thickness and refractive index of the remaining overlays) were varied one at a time to study their effect on the response.

3.1 One-layer sensor

As mentioned in the introduction, the one-layer sensor has been studied quite thoroughly in literature. However, it seems justified to repeat a few basic observations as the following sections will build on these principles. In Figure 2 a) a plot of the mode structure of the fiber with an overlay of $1 \mu\text{m}$ is shown. It can be seen that as long as the overlay refractive index is lower than that of the cladding, there is no transition of modes into the overlay. This is not surprising, as in this case the field would decay exponentially in the radial direction within the overlay. However, even if the overlay refractive index is higher than that of the cladding there is still a certain minimum thickness required to get transitions. This can be seen in Figure 2 b), where the mode structure of a fiber with an overlay with a refractive index of 1.5 and increasing thickness is shown. As the overlay thickness increases, an increasing number of transitions are found, reflecting the increasing number of modes that can be guided in the overlay. It appears that the refractive index interval of the transition increases with the mode order and the number of the transition. From the plots it can also be seen that the transitions of higher order modes start at a lower refractive index than those of the lower order modes.

These trends are explicable considering that the refractive index interval in which the transition will take place should depend on how well the mode can be confined in the overlay. From this it follows that each new transition should occur in an interval that is slightly larger than the one before. Furthermore, the effective refractive index of higher order modes is lower and they should therefore be able to extend further into overlays with lower refractive index, which explains the onset of the transitions at lower overlay refractive indices.

Furthermore, it can be seen that the increase in thickness and the increase of the refractive index of the coating yield similar effects. On one hand, this is a disadvantage as possible swelling of the polymer may cause interferences. On the other hand, it can be an advantage as lack of control of one parameter of the polymer (either refractive index or thickness) can be compensated by better control over the other parameter.

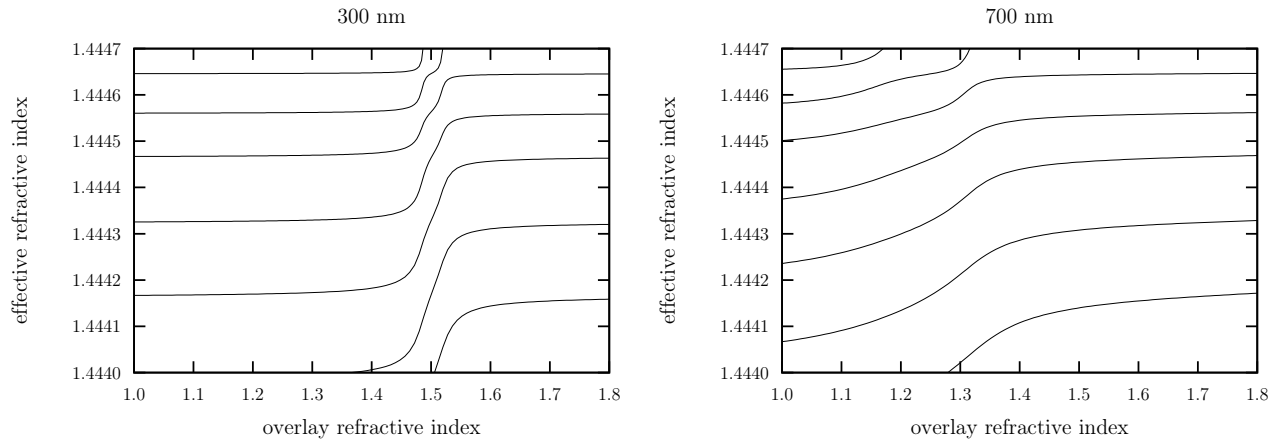


Figure 3. Mode structure of a fiber with two overlays. The refractive index of the inner layer is 1.5, while its thickness is given in the title of the plots. The outer layer has a thickness of 500 nm. The numbers of the abscissa refer to the refractive index of the outer layer.

3.2 Two-layer sensor

With two overlays there are four parameters (thickness and refractive index of each overlay) to vary. Plotting the refractive index of the second (outer) overlay on the abscissa again, there are three parameters left to investigate. However, a few configurations should resemble what was already established in the case of one overlay. If both overlays have a refractive index smaller than that of the cladding, the behavior should be similar to an LPG coated with only one low refractive index overlay. If the first layer has a refractive index higher than that of the cladding and higher than that of the second layer, it will act as a guiding structure. The second layer will, depending on its refractive index and thickness, contribute to the guiding effect. Should the refractive index of the second layer be higher than of the cladding and also than that of the first layer, two cases have to be distinguished. First, the inner overlay can have a refractive index larger than that of the cladding and therefore contribute to the guidance. Second, the refractive index of the first coating can be smaller than that of the cladding, in which case it would act as a barrier.

The following analysis will corroborate and extend work found in the literature. Del Villar *et al.* reported¹⁵ that the sensitivity of an LPG with a high refractive index overlay is enhanced when the refractive index of the overlay is just larger than that of the cladding. In this work, overlays with a refractive index lower than that of the cladding will be considered as well and their utility in combination with a high refractive index overlay will be shown. This configuration was independently suggested by del Villar,²¹ but not investigated in detail. Furthermore, del Villar *et al.*¹⁴ found that the limitation of single high refractive index overlays, which are only sensitive to refractive indices higher than that of the cladding, can be overcome by using an inner high refractive index overlay and an outer low refractive index overlay. The existing work will be put into context and it will be shown how the sensitivity and dynamic range can be tuned over a broad range.

Since the refractive index of the second layer was always varied over the interval 1.0-1.8, only the two cases described at the beginning of this section needed to be investigated. In the first case, the refractive index of the first layer is higher than that of the cladding while in the second case it is lower. As can be seen in Figure 3, an increase in thickness causes the transitions to take place at smaller refractive indices of the second overlay. It is worth noting that, even though one transition can move out of the refractive index range of interest on the low side, another comes into the range of interest if the thickness of the first overlay is further increased. Furthermore, it is apparent that the transition occurs over a larger refractive index interval. The observed displacement of the transition enables the positioning of the interval of highest sensitivity at any given refractive index interval of the second overlay. However, as the transition is displaced, the magnitude of the interval it covers also changes. Varying the refractive index of the inner overlay instead of its thickness, the effects observed are qualitatively the same.

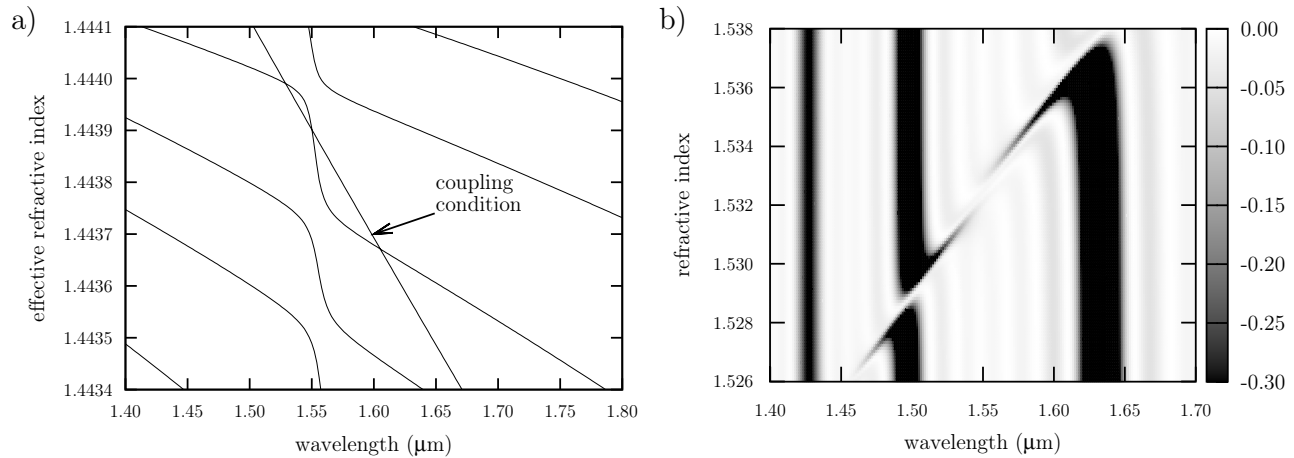


Figure 4. a) Plot of the mode structure versus wavelength of a fiber with two overlays. The refractive index of the inner layer is 1.2 and its thickness 500 nm. The outer layer has a refractive index of 1.5325 and thickness of 1000 nm. b) Plot of the spectrum in the wavelength interval of 1.4-1.7 μm versus the refractive index of the second overlay. The color key refers to the transmittance and was cut-off at -0.3 dB to show low intensity resonances better. The actual minimum transmittance was about -1.2 dB.

The case of the refractive index of the inner layer being lower than that of the cladding is really just the continuation of the trend already discussed. As the refractive index of the first layer gets lower, the transition occurs in a smaller interval, translating into higher sensitivity. However, the interval of highest sensitivity is also moved to higher refractive indices. In the study so far, it was always assumed that the slope of the line representing the coupling condition in a plot of the mode structure versus wavelength is much steeper than that of the mode transitions. Therefore, the line of each mode and the line representing the coupling condition would have at most one intersection, meaning that the cladding mode would couple strongly with the core mode at only one wavelength. As a result, each mode would at most have one corresponding peak in a given spectrum. Introducing a barrier layer however, a situation can be imagined where this is no longer true. If the slope of the mode transitions becomes steeper than the slope of the line representing the coupling condition, it is possible that the lines intersect more than once. This situation is illustrated in Figure 4 a). As a consequence, one mode can give rise to more than one peak. As the refractive index of the second overlay changes, the mode structure can be imagined to shift laterally. The resulting spectra can be easily imagined and an example is shown in Figure 4 b). It can be seen that the position of the original peaks change little. However, the intensity of the peak at about 1500 nm drops in intensity in a small refractive index interval and, as the refractive index increases, an additional peak appears and moves between two of the original peaks. As the character of the mode changes from an odd to an even mode during this transition, the peak diminishes in intensity. In the center of the transition, the peak disappears and shortly after a new peak appears. This peak increases in intensity and shifts further until it unites with one of the original peaks. As the refractive index of the second layer increases, similar effects can be seen for the mode of the next higher order.

These novel effects have obvious uses for the development of new sensors. Using this approach, the sensitivity of the sensor can be increased considerably. Furthermore, the prediction of two peaks in the spectrum corresponding to the same mode potentially opens up the road to new detection schemes using one peak as a reference or internal standard.

A disadvantage of the two layer sensor as presented in this section is that either the location or the range of the refractive index response can be specified. However, for sensor applications it would be desirable to adjust both properties of the sensing element at the same time. In the next section, a possible route for the optimization of sensitivity and dynamic range in the same LPG element will be shown.

3.3 Three-layer sensor

As shown in the previous section, the two-layer sensor allows for the adjustment of either the position of the RI response region or its dynamic range/sensitivity. For many applications, this will allow sufficient control over the response of the LPG to design a good sensor. In other cases, more optimization might be required. The work on the three-layer sensor was motivated by the desire to control the position of the transition in the case of having an inner overlay with a refractive index lower than that of the cladding (i.e. having a transition occurring in a very small refractive index interval). A similar problem has already been encountered in the case of a single overlay¹⁴ and the same solution (i.e. the introduction of an additional layer) proved to provide a suitable solution. Having three layers provides a very high degree of customizability. The structure can be thought of a combination of the two different cases of two-layer sensors described in the last section, where the second layer of the first structure and the first layer of the second structure coincide to form a middle layer. The middle overlay will generally have the highest refractive index (certainly higher than that of the cladding) and therefore provides a second region where modes can be guided.

If the inner overlay has a lower refractive index than the cladding, it will act as a barrier, separating the cladding from the middle overlay. This barrier will determine the magnitude of the refractive index interval for the transition. Lowering the refractive index or increasing the thickness of the inner overlay will lead to a smaller transition interval and therefore higher sensitivity. The two outer overlays will provide the guiding structure. Again, both the radius and the refractive index of the overlays can be used to obtain a set-up with suitable characteristics. It should be noted that, given enough control over properties of the middle layer, the refractive index of the outer overlay can be freely chosen and there are few restraints on the radius. Therefore, the third layer can be optimized for chemical selectivity with little regard for its optical properties.

One of the main advantages of the three-layer structure is the ability to adjust the transition interval and position independently from the chemical selectivity. A problem might, of course, be the production and stability of a fiber structure with three different overlays. In tackling this daunting task it might be helpful to consider that — as pointed out with the one-layer sensor — different choices of parameters can yield very similar response characteristics. If it is possible to control either the layer thickness or its refractive index very well, the lack of control over the other parameter can be compensated in many situations.

3.4 Case study

To demonstrate the benefits of the proposed multi-layer sensors, an example from literature was chosen as a case study. Giordano *et al.*²⁴ described an optical sensor for chloroform vapors using a polystyrene film as the transducer. In their work, the change of the refractive index of the polymer film caused by the absorption of chloroform was studied in detail. The refractive index of the polymer given was 1.5781 at 25° at 1310 nm. In the paper, the refractive index change at the maximum concentration of chloroform in the polymer (about 6.5 g of chloroform per 100 g of polymer) was reported to be about 0.014. Based on this work, an attempt was made to design an LPG sensor that would cover the refractive index range of interest. To allow the use of a simple detection scheme, intensity changes at a single wavelength were monitored in the simulations.

The simplest solution is a single layer sensor. Since the refractive index of the overlay was fixed, the only parameter left to optimize was the layer thickness. The result for the ideal thickness of 370 nm is shown in Figure 5 a). The three spectra shown correspond to the refractive indices of the polymer and the polymer with 50% and 100% of the maximum chloroform loading investigated in the paper. It can be seen, that the resulting spectrum is fairly complex due to the transitions the different peaks experience. The easiest peak to monitor was the resonance at about 1.6 μm . However, it was difficult to select a single wavelength that would allow the monitoring of the refractive index over the whole range desired. The wavelength selected for this study was 1.59 μm as indicated in Figure 5 a). In Figure 5 d) a plot of the change of transmittance at the wavelength chosen versus the change of refractive index is shown with the label “original”. It can be seen that the response of this sensor presents several challenges for the data analysis. The curve is highly non-linear, yielding a different sensitivity in different refractive index intervals. Furthermore, the transmittance decreases over most of the refractive interval, but then increases at high concentrations, as the center of peak moves past the selected wavelength. In this case, two different concentrations yield the same response and are therefore indistinguishable.

Using the single layer sensor described in the preceding paragraph as a baseline, a total of three improved sensors were simulated. The first sensor was designed to have an almost linear response over the whole refractive index interval of interest. To achieve this result, a two-layer design was chosen. The refractive index of the first layer was 1.48 and its thickness was 450 nm. The refractive index of the second layer was again predetermined by the chemically selective coating and its thickness was 250 nm. The spectra are not shown, since they are very similar to the ones of the original sensor. A plot of the transmittance change versus the refractive index change is shown in Figure 5 d) labeled “linear range”. It can be seen that although the sensitivity is reduced as compared to the first sensor, this new design has the advantage of having an almost linear and monotonic response over the whole refractive index range of interest.

For the second sensor, a barrier layer was introduced. The geometry includes an inner layer with a refractive index of 1.27 and a thickness of 600 nm. The second layer has a refractive index of 1.5 and a thickness of 919 nm. The thickness of the outermost layer was 300 nm. The corresponding spectra are shown Figure 5 b). It is apparent that in this case only one peak undergoes significant changes. With this sensor, the intensity change in the peak at 1.65 μm was measured as it reappeared in the spectrum. The resulting transmittance change is plotted in Figure 5 d) and labeled “sensitivity/range”, indicating that, although the response is nonlinear, it is monotonic and covers the entire range, with the highest sensitivity at the lowest concentration, often a desirable feature. The drawback of this design is that the sensitivity cannot be adjusted, since it is determined by the wavelength dependence of the refractive index of the fiber and polymer materials. This design deserves some attention due to the fact that there is hardly any change in the position of the peak. The change in intensity is almost entirely due to the reappearance of the peak. The sensitivity is highest at small refractive index changes, and then diminishes with increasing refractive index change, but in contrast to the cases where the peak shift caused the intensity change, the intensity approaches a maximum and then remains constant. Only if the refractive index is increased enough to trigger another transition will the peak change again. Furthermore, it can be seen that the lower order peaks do not change significantly and can therefore be used as a reference indicating, for example, changes in temperature or other interferences.

The third sensor was designed to provide very high sensitivity in a limited refractive index interval (in this case the first 10% of the original interval). The geometry of this sensor is almost identical to the last one, only the second layer was increased to 931 nm. This time however, the shift of the side peaks was monitored as shown in Figure 5 c). Due to this change in inquiring the sensor element, a very different response is obtained. As can be seen in Figure 5 d) with the data series labeled “sensitivity”, the sensitivity was highly increased. It was also possible to tune the response to obtain an almost linear increase in transmittance over the refractive interval desired.

4. CONCLUSIONS

It has been demonstrated in literature that thin coatings can considerably enhance the sensitivity of LPGs and allow the refractive index interval of highest sensitivity to be tuned to some extent. In this report, the literature findings were put into context and the selection of configurations was extended. The benefits of overlay structures with inner coatings of low refractive index for high sensitivity sensing were shown. Novel and interesting spectral responses of these structures were predicted. An explanation of the response was provided considering the change of the mode structure with wavelength and its use for sensing applications was illustrated. Furthermore, the advantages of three overlay setups for more flexibility in tuning of the response of the optical element were explored. It was demonstrated that with a maximum of three layers, the dynamic range as well as the refractive index interval of highest sensitivity can be tuned over a broad range with few restrictions. It was found that the tuning of different properties (sensitivity, region of highest sensitivity) can be separated to some extent and that often one property is affected most by one specific layer. Therefore, different parameter sets can be used to obtain very similar responses, which lowers the requirements in terms of control over the refractive index, the thickness and the chemical selectivity of a particular layer. This flexibility in the choice of coating parameters should make it easier to produce the required multi-layer structures. It should also be possible to accommodate certain restrictions on the choice of the parameters imposed by chemical or physical properties of a particular material. The results presented in this report can be used as a framework for the rational tuning of the response of LPGs even if the selection of some parameters is restricted. The immediate utility of this investigation was

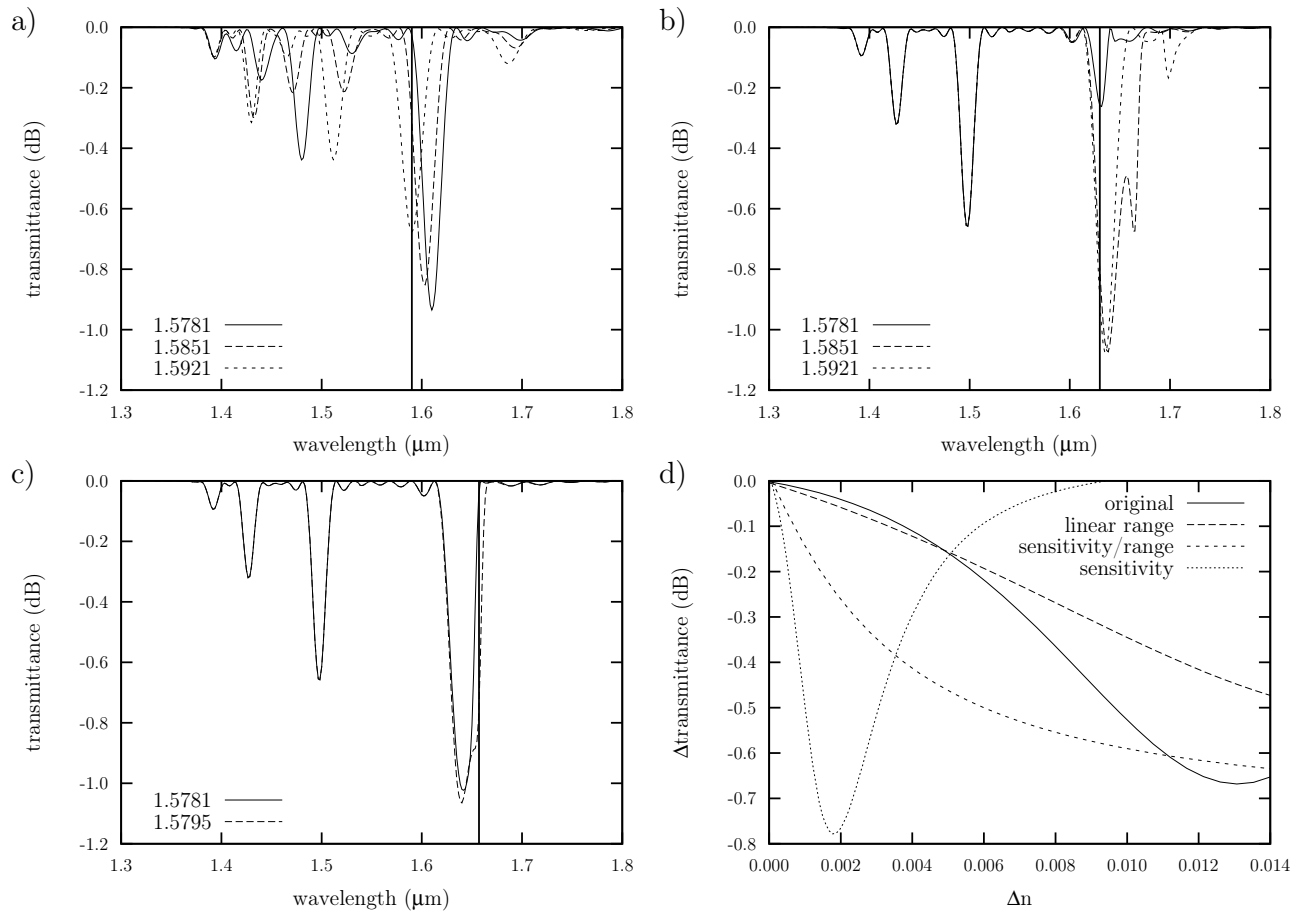


Figure 5. Simulated spectra at different refractive indices for three sensor designs: a) one-layer, b) and c) three-layer (see text for design details). Panel d) Plot of the change of the transmittance versus the change in refractive index for the four sensors described in the text.

demonstrated by proposing optimized designs in a case study based on a sensor for chloroform presented in literature.

ACKNOWLEDGEMENTS

The authors gratefully acknowledge the financial support of Precarn Inc., the Dalhousie University Killam Trust and the Natural Science and Engineering Research Council (NSERC).

REFERENCES

1. S. W. James and R. P. Tatam, "Optical fibre long-period grating sensors: characteristics and application," *Meas. Sci. Technol.* **14**, pp. R49–R61, 2003.
2. N. D. Rees, S. W. James, R. P. Tatam, and G. J. Ashwell, "Optical fiber long-period gratings with langmuir-blodgett thin-film overlays," *Opt. Lett.* **27**, pp. 686–688, 2002.
3. A. Cusano, P. Pilla, L. Contessa, A. Iadicicco, S. Campopiano, A. Cutolo, M. Giordano, and G. Guerra, "High-sensitivity optical chemosensor based on coated long-period gratings for sub-ppm chemical detection in water," *Appl. Phys. Lett.* **87**, p. 234105, 2005.
4. J. Barnes, R. S. Brown, C. M. Crudden, M. Dreher, K. Plett, and H.-P. Loock, "Chemical sensor based on a functionalized polydimethylsiloxane coated-long-period fiber grating," *Anal. Chem.* submitted, 2007.
5. S. W. James and R. P. Tatam, "Fibre optic sensors with nano-structured coatings," *J Opt. A-Pure Appl. Op.* **8**, pp. S430–S444, 2006.
6. I. M. Ishaq, A. Quintela, S. W. James, G. J. Ashwell, J. M. Lopez-Higuera, and R. P. Tatam, "Modification of the refractive index response of long period gratings using thin film overlays," *Sensor. Actuat. B-Chem.* **107**, pp. 738–741, 2005.
7. I. del Villar, M. Achaerandio, I. R. Matías, and F. J. Arregui, "Deposition of overlays by electrostatic self-assembly in long-period fiber gratings," *Opt. Lett.* **30**, pp. 720–722, 2005.
8. I. del Villar, I. R. Matías, F. J. Arregui, and P. Lalanne, "Optimization of sensitivity in long period fiber gratings with overlay deposition," *Opt. Express* **13**, pp. 56–69, 2005.
9. I. del Villar, I. R. Matias, F. J. Arregui, and M. Achaerandio, "Nanodeposition of materials with complex refractive index in long-period fiber gratings," *J. Lightwave Technol.* **23**, pp. 4192–4199, 2005.
10. Z. Wang, J. R. Heflin, R. H. Stolen, and S. Ramachandran, "Sensitive optical response of long period fiber gratings to nm-thick ionic self-assembled multilayers," *Proceedings of the Conference on Lasers and Electro-Optics (CLEO '04)* **1**, pp. 1259–1260, 2004.
11. Z. Wang, J. R. Heflin, R. H. Stolen, and S. Ramachandran, "Highly sensitive optical response of optical fiber long period gratings to nanometer-thick ionic self-assembled multilayers," *Appl. Phys. Lett.* **86**, p. 223104, 2005.
12. Z. Wang, J. R. Heflin, R. H. Stolen, and S. Ramachandran, "Analysis of optical response of long period fiber gratings to nm-thick thin-film coatings," *Opt. Express* **13**, pp. 2808–2813, 2005.
13. I. del Villar, I. R. Matias, and F. J. Arregui, "Influence on cladding mode distribution of overlay deposition on long-period fiber gratings," *J. Opt. Soc. Am. A* **23**, pp. 651–658, 2006.
14. I. del Villar, I. R. Matias, and F. J. Arregui, "Enhancement of sensitivity in long-period fiber gratings with deposition of low-refractive-index materials," *Opt. Lett.* **30**, pp. 2363–2363, 2005.
15. I. del Villar, I. R. Matias, and F. J. Arregui, "Long-period fiber gratings with overlay of variable refractive index," *IEEE Photonic. Tech. L.* **17**, pp. 1893–1895, 2005.
16. A. Cusano, A. Iadicicco, P. Pilla, L. Contessa, S. Campopiano, A. Cutolo, and M. Giordano, "Cladding mode reorganization in high-refractive-index-coated long-period gratings: effects on the refractive-index sensitivity," *Opt. Lett.* **30**, pp. 2536–2538, 2005.
17. A. Cusano, A. Iadicicco, P. Pilla, L. Contessa, S. Campopiano, A. Cutolo, M. Giordano, and G. Guerra, "Coated long-period fiber gratings as high-sensitivity optochemical sensors," *J. Lightwave Technol.* **24**, pp. 1776–1786, 2006.
18. A. Cusano, A. Iadicicco, P. Pilla, L. Contessa, S. Campopiano, A. Cutolo, and M. Giordano, "Mode transition in high refractive index coated long period gratings," *Opt. Express* **14**, pp. 19–34, 2005.

19. A. Cusano, A. Iadicicco, P. Pilla, A. Cutolo, M. Giordano, and S. Campopiano, "Sensitivity characteristics in nanosized coated long period gratings," *Appl. Phys. Lett.* **89**, p. 201116, 2006.
20. E. Anemogiannis, E. N. Glytsis, and T. K. Gaylord, "Transmission characteristics of long-period fiber gratings having arbitrary azimuthal/radial refractive index variations," *J. Lightwave Technol.* **21**, pp. 218–227, 2003.
21. I. del Villar, *Theoretical analysis and fabrication of nanostructures with Electrostatic Self-Assembly Monolayer process*. PhD thesis, Universidad Pública de Navarra, 2006.
22. P. Yeh, A. Yariv, and E. Marom, "Theory of bragg fiber," *J. Opt. Soc. Am.* **68**, pp. 1196–1201, 1978.
23. T. Erdogan, "Cladding-mode resonances in short- and long-period fiber grating filters," *J. Opt. Soc. Am. A* **14**, pp. 1760–1773, 1997.
24. M. Giordano, M. Russo, A. Cusano, and G. Mensitieri, "An high sensitivity optical sensor for chloroform vapours detection based on nanometric film of δ -form syndiotactic polystyrene," *Sensor. Actuat. B-Chem.* **107**, pp. 140–147, 2005.